ChemPubSoc Europe

DOI: 10.1002/ejic.201501075

EurJIC European Journal of Inorganic Chemistry

Full Paper

CLUSTER ISSUE

Phosphathioethynolates

Ambient-Temperature Synthesis of 2-Phosphathioethynolate, PCS^-, and the Ligand Properties of ECX^- (E = N, P; X = O, S)

Andrew R. Jupp,[a] Michael B. Geeson,[a] John E. McGrady,[a] and Jose M. Goicoechea*[a]

Abstract: A synthesis of the 2-phosphathioethynolate anion, PCS^-, under ambient conditions is reported. The coordination chemistry of PCO^-, PCS^- and their nitrogen-containing congeners is also explored. Photolysis of a solution of $W(CO)_6$ in the presence of PCO^- [or a simple ligand displacement reaction using $W(CO)_5(MeCN)$] affords $[W(CO)_5(PCO)]^-$ (**1**). The cyanate and thiocyanate analogues, $[W(CO)_5(NCO)]^-$ (**2**) and $[W(CO)_5(NCS)]^-$ (**3**), are also synthesised using a similar methodology, allowing for an in-depth study of the bonding properties of this family of related ligands. Our studies reveal that, in the coordination sphere of tungsten(0), the PCO^- anion preferentially binds through the phosphorus atom in a strongly bent fashion, while NCO^- and NCS^- coordinate linearly through the nitrogen atom. Reactions between PCS^- and $W(CO)_5(MeCN)$ similarly afford $[W(CO)_5(PCS)]^-$; however, due to the ambidentate nature of the anion, a mixture of both the phosphorus- and sulfur-bonded complexes (**4a** and **4b**, respectively) is obtained. It was possible to establish that, as with PCO^-, the PCS^- ion also coordinates to the metal centre in a bent fashion.

Introduction

Multiple bonds involving elements with a principal quantum number greater than two were once thought to be inaccessible under the tenets of the double bond rule.[1,2] This theory has since been thoroughly disproved, with countless examples of heavier main group systems containing multiple bonds that are kinetically and thermodynamically stabilised by substituents with high steric bulk.[3] For example, the diphosphene and the phosphaalkene pictured in Figure 1 can both be stabilised by large aromatic groups.[4–7] Even formal P≡C triple bonds are stable when sterically encumbering substituents are employed, for example in phosphaalkynes.[8]

By contrast, examples of multiply bonded main group element systems that are not sterically protected by bulky substituents are much rarer. One such case is the 2-phosphaethynolate anion, PCO^-, the phosphorus analogue of cyanate, first synthesised as a lithium salt by Becker in 1992.[9] In this species, stabilisation of the P–C multiple bond is a consequence of negative charge delocalisation along the anion. This precludes common decomposition pathways such as oligomerisation (available to related species such as phosphaalkynes), because of electrostatic repulsion between monomers. Nevertheless, lithium salts of PCO^- have significant covalent character, leading to a decrease in formal negative charge on the PCO^- moiety. Consequently, $[Li(dme)_2][PCO]$ (dme = 1,2-dimethoxyethane) was found to be very sensitive to decomposition. Accordingly, very few accounts of the reactivity of the 2-phosphaethynolate anion were reported in the twenty years following its discovery.[10,11]

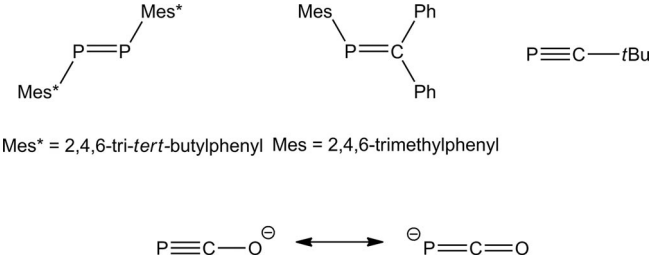

Figure 1. Selected examples of systems with multiple bonds to phosphorus, and resonance forms of PCO^-.

There has been renewed interest in the 2-phosphaethynolate anion over the last four years, stimulated primarily by novel and facile synthetic routes, which enable its isolation on multigram scales.[12,13] These preparations yield the sodium and potassium salts, which are more ionic in nature and consequently more stable with respect to decomposition. There have been numerous reports of the use of the 2-phosphaethynolate anion as a precursor to original organophosphorus derivatives,[14–16] phosphorus-containing heterocycles,[12,17–21] and as a phosphide-transfer reagent.[22–24]

A recent report on tris(amidinate) actinide (Th, U) complexes of PCO^- revealed an oxygen-bound terminal phosphaethynolate, whereas both the NCO^- and NCS^- analogues favoured

[a] Department of Chemistry, University of Oxford, Chemistry Research Laboratory
12 Mansfield Road, Oxford OX1 3TA, UK
E-mail: jose.goicoechea@chem.ox.ac.uk
http://research.chem.ox.ac.uk/jose-goicoechea.aspx

Supporting information for this article is available on the WWW under http://dx.doi.org/10.1002/ejic.201501075.

nitrogen coordination.[25] This is attributed to the largely ionic nature of the bonding; as a result the E/X atom (E = N, P; X = O, S) with the greater negative partial charge preferentially binds to the actinide centre. This is in accord with a previous spectroscopic and computational study exploring the ambidenticity of the phosphaethynolate anion.[26]

The groups of Grützmacher and Peruzzini have synthesised the only known transition metal complex of PCO^- to date (reported alongside the cyanate analogue for comparison), in the form of [Re(η^1-ECO)$(CO)_2$(triphos)] (E = N, P; Figure 2).[27] In contrast to the actinide complexes, the two ECO^- ligands both bind through the pnictogen atom, but in this case with different coordination geometries. The PCO^- ligand coordinates in a strongly bent manner, with a Re–P–C bond angle of approximately 90°, whereas NCO^- binds almost linearly and the Re–N–C bond angle approaches 180°. This was corroborated by computational calculations and is not merely an effect of crystal packing; however, crystallographic disorder in both rhenium structures precludes an accurate discussion of bond metric data. IR spectroscopy revealed that, despite this profound difference in coordination geometry, both ECO^- ligands "*exert indistinguishable effects on the [Re$(CO)_2$(triphos)] fragment.*"

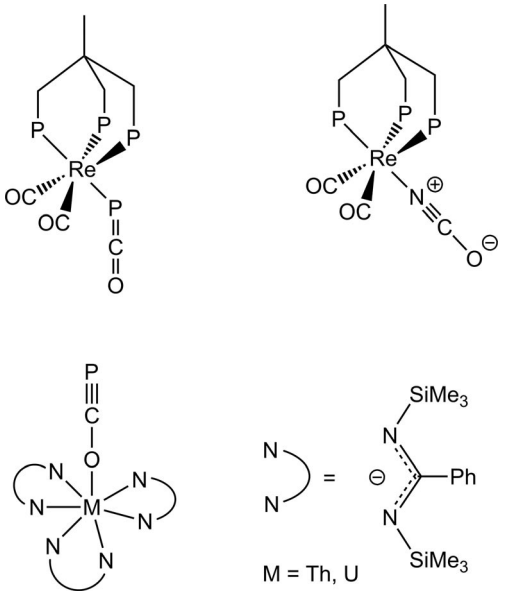

Figure 2. Known coordination complexes of PCO^-, and a NCO^- analogue.

The aforementioned studies prompted us to carry out a more extensive exploration of the ligand properties of PCO^- compared to those of NCO^-. The metal complexes chosen for carrying out this analysis were those derived from the $W(CO)_5$ fragment. Many reactive species have been trapped and stabilised in the coordination sphere of this moiety, and as a result $W(CO)_5$(L) complexes have been used as a benchmark for a multitude of experimental and computational ligand studies in the past, allowing a thorough comparison to other systems. From a practical perspective, the tungsten(0) centre is stable to reduction by the relatively reactive PCO^-, a phenomenon which has previously plagued the coordination chemistry of this ligand.[27]

Results and Discussion

Coordination Studies of PCO^- and NCX^- (X = O, S)

Photolysis of a THF solution of $W(CO)_6$ and [K(18-crown-6)][PCO] led to the formation of [K(18-crown-6)][$W(CO)_5$(PCO)] ([K(18-crown-6)][**1**]). This product could also be obtained more cleanly by simple displacement of the labile acetonitrile ligand of $W(CO)_5$(MeCN). The coordinated product, **1**, displayed a singlet at δ = –439.3 ppm, 44 ppm upfield of free PCO^-, in the ^{31}P NMR spectrum.

The most striking feature of the ^{31}P NMR spectrum of **1** is the magnitude of the ^{183}W satellites (^{183}W: 14.3 % abundant, I = 1/2), which is only 51.9 Hz (Figure 3). This value is too large to result from a three-bond scalar coupling, as would be anticipated for oxygen-bound PCO^-. Therefore, it must be due to a one-bond coupling arising from phosphorus coordination; however, typical $^1J_{P\text{-}W}$ coupling constants are of the order of 250 Hz. We believe that our recorded value is small, because bonding to the tungsten metal centre predominantly occurs through one of the phosphorus p orbitals. The Fermi-contact mechanism is crucially dependent on the s character of the bond, as only the s orbitals have a non-zero probability of having electron density at the nucleus. This would be the case if PCO^- was bound in a side-on manner with a W–P–C bond angle of approximately 90°, in an analogous manner to the rhenium structure reported by Grützmacher, Peruzzini and co-workers. The lone pair on phosphorus for this compound was calculated to have very high s character (68 %).[27] This low $^1J_{P\text{-}W}$ coupling constant can therefore be perceived as a spectroscopic indicator of side-on bonding.

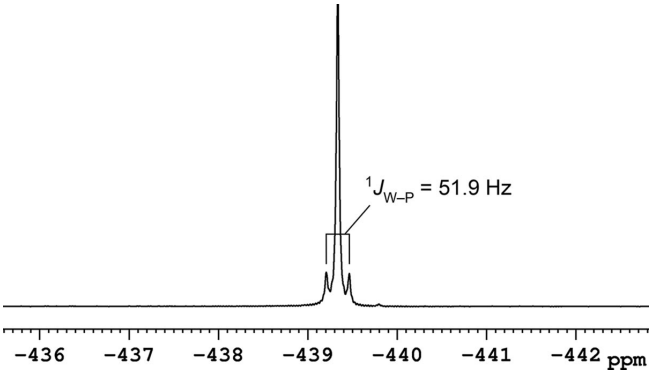

Figure 3. ^{31}P NMR spectrum of [K(18-crown-6)][**1**] showing ^{183}W satellites.

The proposed bonding mode was confirmed by single-crystal X-ray diffraction studies. Large, yellow, block-shaped crystals were grown by slow diffusion of hexane into a THF solution of [K(18-crown-6)][**1**], and the crystallographic analysis clearly shows PCO^- to be bound through the phosphorus atom in a bent geometry. Unfortunately, crystallographic disorder causes the PCO^- moiety to be disordered over two positions *trans* to one another, with the carbonyl group occupying the other position 50 % of the time. This precludes the accurate analysis of bond metric data, particularly the W–C bond length *trans* to the PCO^- anion, which is one of the parameters we were most interested in to probe the properties of the ECO^- ligands.

The analogous compound [K(18-crown-6)][$W(CO)_5$(NCO)] ([K(18-crown-6)][**2**]) was synthesised and crystallised in a similar manner. Although this anion has long been known, commonly synthesised by the reaction of tungsten–hexacarbonyl with an azide salt, previously it has only been characterised spectroscopically.[28–32] [K(18-crown-6)][**2**] did not exhibit any crystallographic disorder and revealed the NCO^- to be nitrogen-bound in an almost linear fashion.

To extend this study we also synthesised the thiocyanate complex, [K(18-crown-6)][$W(CO)_5$(NCS)] ([K(18-crown-6)][**3**]). This anion has also been studied spectroscopically; however, to the best of our knowledge, no crystal structure for it has been reported to date. NCS^- is an archetypal ambidentate ligand; it is able to bind through either the nitrogen or the sulfur centre depending on the metal in question. Previous IR spectroscopic studies on the $[W(CO)_5(NCS)]^-$ anion suggested that the ligand is nitrogen-bound in this complex.[33,34] This is due to the decrease in charge on the metal centre compared to that for the isoelectronic Mn^I complex, in which the ligand is bound through the sulfur atom.[35] The crystal structure of [K(18-crown-6)][**3**] confirms that the ligand is nitrogen-bound in an end-on manner.

[K(18-crown-6)][**1**] exhibited extensive crystallographic disorder, and hence the structure was not suitable for a discussion of bond metrics; therefore, both **1** and **2** were synthesised by using different counter-cations. An exchange of the potassium-sequestering agents led to the formation of [K(2,2,2-crypt)][$W(CO)_5$(ECO)] {E is P for [K(2,2,2-crypt)][**1**] and N for [K(2,2,2-crypt)][**2**]}. Both of the structures determined by single-crystal X-ray diffraction were free from any disorder phenomena, and this enabled a comparative evaluation of their bond metric data (Table 1).

Table 1. Selected experimental bond lengths (Å) and bond angles (°).

	1	**2** (crown salt)	**2** (crypt salt)	**3**
W1–E1	2.666(1)	2.183(3)	2.193(2)	2.180(2)
E1–C1	1.616(4)	1.159(4)	1.156(4)	1.157(4)
C1–X1	1.176(5)	1.209(4)	1.221(4)	1.648(3)
$W1–C_{trans}$[a]	1.969(3)	1.960(3)	1.969(3)	1.966(3)
$C–O_{trans}$[b]	1.161(4)	1.164(4)	1.155(3)	1.147(5)
$W1–C_{cis}$[c]	2.057(av)	2.047(av)	2.044(av)	2.046(av)
$C–O_{cis}$[d]	1.123(av)	1.138(av)	1.140(av)	1.137(av)
W1–E1–C1	94.7(1)	172.9(2)	170.0(2)	169.6(2)
E1–C1–O1	176.8(4)	177.1(3)	179.3(3)	177.4(3)

[a] W1–C2. [b] C2–O2. [c] Average (av) of W1–C3, W1–C4, W1–C5 and W1–C6. [d] Average (av) of C3–O3, C4–O4, C5–O5 and C6–O6.

The identity of the cation makes very little difference to the structure of the anion for the two cyanate complexes, [K(18-crown-6)][**2**] and [K(2,2,2-crypt)][**2**], as all of the bond lengths were found to be identical within statistical error. Therefore, the discussion will focus on the differences between the two $[K(2,2,2\text{-crypt})]^+$ salts, [K(2,2,2-crypt)][**1**] and [K(2,2,2-crypt)][**2**]. The W1–E1–C1 bond angles clearly show the aforementioned side-on nature of the PCO^- binding [94.7(1)°], while the NCO^- is bound end-on [170.0(2)°]. The P1–C1 bond length increases from 1.579(3) Å in free [K(18-crown-6)][PCO] to 1.616(4) Å in the coordinated complex, and the corresponding (P1)C1–O1 bond length decreases from 1.212(4) Å to 1.176(5) Å upon coordination.[12] In contrast, the coordinated cyanate ion in **2** has a significantly longer C1–O1 bond length of 1.221(4) Å and a short N1–C1 bond length of 1.156(4) Å (cf. 1.219(5) and 1.128(5) Å, respectively, in $[NMe_4][OCN]$).[36] This is consistent with the bonding model proposed by Grützmacher, Peruzzini and co-workers for the rhenium complexes.[27] While [K(2,2,2-crypt)][**1**] resembles a metallaphosphaketene with an allene-like O=C=P^- moiety, [K(2,2,2-crypt)][**2**] contains a cyanate anion, which is better described as having a contribution from a N≡C–O^- resonance structure in addition to that from the expected O=C=N^-. These bonding models are further supported by looking at the interactions of the bound ECO^- ligands with the counter-cation, $[K(2,2,2\text{-crypt})]^+$. This sequestering agent is well documented to strongly encapsulate K^+, and accordingly there is no interaction between the O1 atom of the PCO^- moiety in [K(2,2,2-crypt)][**1**] and the K^+ centre. However, in [K(2,2,2-crypt)][**2**], the ligand oxygen atom would formally bear a partial negative charge if the zwitterionic $[M^+–N≡C–O^-]^-$ structure were a valid resonance contribution. This appears to be the case and results in a sufficiently strong electrostatic cation/anion interaction to splay open the 2,2,2-crypt (see Figure 4).

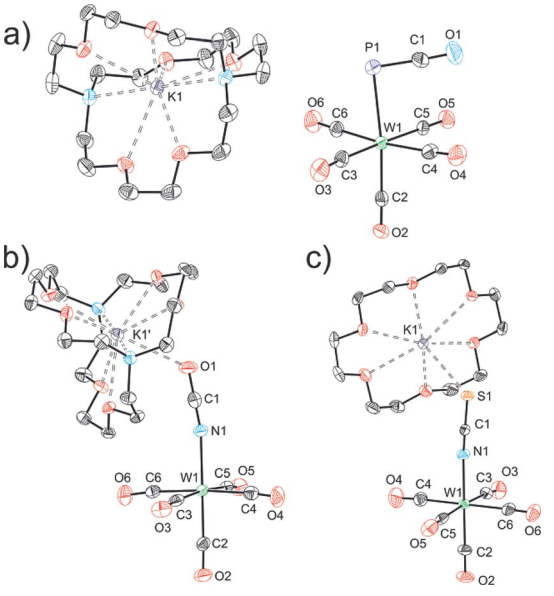

Figure 4. Molecular structures of: (a) [K(2,2,2-crypt)][**1**], (b) [K(2,2,2-crypt)][**2**] and (c) [K(18-crown-6)][**3**]. Anisotropic displacement ellipsoids are pictured at 50 % probability. All hydrogen atoms are omitted for clarity.

The bond metric data for [K(18-crown-6)][**3**] are very similar to those of [K(18-crown-6)][**2**]. This implies that the nitrogen-bound NCO^- and NCS^- ligands coordinate in a similar manner; the NCS^- ligand binds end-on with contributions from the two different resonance structures described above. There was no evidence for sulfur-bound NCS^- coordination products in any of the experiments carried out.

The W1–P1 bond in [K(2,2,2-crypt)][**1**] is remarkably long [2.666(1) Å]. A search of the CSD for tungsten–pentacarbonyl fragments bearing a phosphorus-bound ligand returned a mean W–P bond length of 2.513 Å and revealed that our value is only slightly shorter than the maximum value of 2.686(4) Å.[37] This latter value is from the tris(*tert*-butyl)-

Table 2. One-bond coupling constants for *cis* and *trans* carbonyl groups (in Hz).

	[K(18-crown-6)][**1**]	[K(18-crown-6)][**2**]	[K(18-crown-6)][**3**]
$^1J_{W\text{-}C(trans)}$	168.6	146.5	147.7
$^1J_{W\text{-}C(cis)}$	125.4	127.8	128.3

phosphine–tungsten–pentacarbonyl complex, $W(CO)_5(PtBu_3)$, where the long bond length primarily arises from the large steric bulk of the phosphine (the Tolman cone angle is 182 ± 2 °).[38,39] In our system, steric constraints are relatively insignificant, and instead the long bond is another manifestation of the fact that the bonding is predominantly p-orbital-based. This is substantiated further by comparison of the $^1J_{P\text{-}W}$ coupling constants between the two species; despite the similar bond lengths, the value for $W(CO)_5(PtBu_3)$ is of a typical magnitude (228.5 Hz).[40] This implies that the low coupling constant for [K(2,2,2-crypt)][**1**] (51.9 Hz) is not a result of the length of the W–P bond, but instead is due to the orbitals involved in bonding to the metal centre.

The *trans* influence, also known as the structural *trans* effect, is a ground-state phenomenon, not to be confused with the kinetic *trans* effect. It is most commonly assessed in terms of the length of the metal–ligand bond *trans* to the ligand in question derived from crystallographic data. The W1–C_{trans} bond length, that is, the bond length *trans* to the ECX^- ligand, is identical [1.969(3) Å] in [K(2,2,2-crypt)][**1**] and [K(2,2,2-crypt)][**2**] and very similar [1.966(3) Å] in [K(18-crown-6)][**3**]. This suggests that the three ligands have the same net electronic properties; however, these experimental data do not allow us to deconvolute the σ and π effects. The W1–C_{cis} bonds are significantly longer than W1–C_{trans} bonds in all cases, which implies that the ECX^- ligands have a weaker *trans* influence than the CO ligands, as expected.

Another useful method of assessing the *trans* influence is available through NMR spectroscopy studies. The $^1J_{W\text{-}C}$ coupling constant of the carbonyl group *trans* to the ECX^- ligand obtained from the ^{13}C NMR spectrum is dependent on the *trans* influence of this ligand, a higher value of $^1J_{W\text{-}C}$ indicating a weaker *trans* influence. The strong W–C bond, strengthened by the large π-accepting ability of the CO ligand, makes it more sensitive to variations in ligand properties and therefore an ideal probe for studying this effect.[41] A study of this type has previously been carried out by Buchner and Schenk, where a range of monosubstituted tungsten–carbonyl complexes, including the NCS^- species, were assessed.[34] The magnitude of a one-bond coupling constant can be taken to reflect the σ-donating ability of the ligand in the *trans* position. If the ECX^- ligand *trans* to a CO makes a lesser demand for the tungsten 6s orbital, then a rehybridisation will occur to increase the contribution from this orbital to the W–C bond. Perturbation theory by Burdett and Albright has shown that the W–C bond will be strengthened if there is an increase in the energy difference between the donor orbitals of the ECX^- ligand and the tungsten acceptor orbital, or if there is a decrease in the overlap integral of the W–E bond.[41]

The coupling constant data are shown in Table 2. As the NMR spectroscopic data of the two salts are similar, only values for the $[K(18\text{-crown-6})]^+$ salts will be discussed (all values are given in the Experimental Section). The coupling constants to the *cis* carbonyl groups vary only to a small degree, which is entirely consistent with previous studies.[34] Thus, when E = P, the values all tend to be approximately 125 Hz, and N-donors give slightly higher values of approximately 130 Hz.

The coupling constants to the *trans* carbonyl groups are more characteristic of the bonding properties of the ECX^- ligand. The value for [K(18-crown-6)][**1**] is significantly higher (168.6 Hz) than those for the two NCX^- complexes (Figure 5). This implies that the PCO^- ligand exerts a weaker *trans* influence, leading to a stronger W–C_{trans} bond and a greater Fermi interaction. In fact, this value is much larger than those for the other phosphorus-based ligands included in prior studies, where typical coupling constants for phosphine ligands are around 140 Hz. From these NMR spectroscopic data, we can infer that PCO^- acts as a weak σ-donor and negligible π-acceptor. By contrast, NCO^- and NCS^- are stronger σ-donors; however, as a result of their increased π-acceptor ability relative to PCO^-, they have a similar net electronic effect, which is manifest in similar W–C_{trans} bond lengths and IR spectra (vide infra).

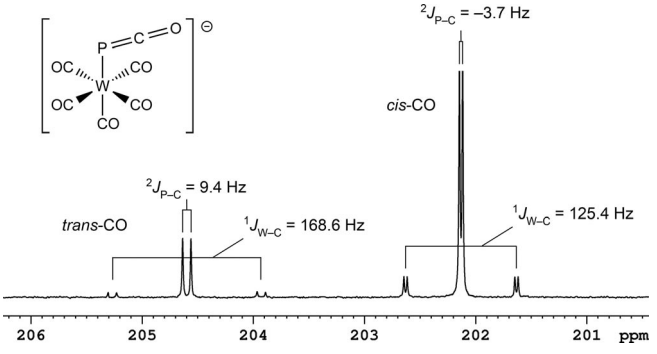

Figure 5. ^{13}C NMR spectrum showing the carbonyl region of [K(18-crown-6)][**1**]. The signs associated with the coupling constants are described in ref.[34]

The 2-Phosphathioethynolate Anion, PCS^-

We sought to extend this study to incorporate the heavier group 16 analogue, PCS^-. The latter was originally synthesised as the lithium salt by Becker in 1994.[42] One of the reported syntheses was the reaction of *O,O'*-diethyl thiocarbonate with lithium bis(trimethylsilyl)phosphide, by analogy with the original preparation of PCO^-.[9] More interesting to us was an alternative synthesis, which entailed the direct reaction of PCO^- with one equivalent of CS_2 to afford PCS^- and OCS, presumably via an undetected cyclic intermediate (Scheme 1). It should be noted that both of these syntheses required the mixing of reagents at −50 °C and yielded sensitive, pale yellow crystals of $[Li(dme)_3][PCS]$.

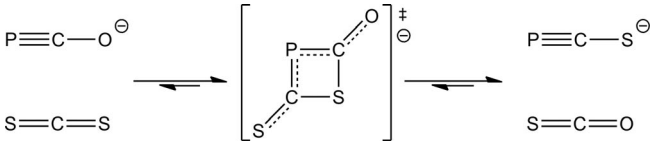

Scheme 1. Formation of PCS^- via a proposed (undetected) cyclic intermediate.

We reasoned that, by analogy with PCO^-, the formation of an alkali metal salt of PCS^- other than that of lithium would make the compound easier to handle and the anion more amenable to further study. This factor, combined with a judicious choice of solvent, allows us to now report the first room-temperature synthesis of PCS^-. [K(18-crown-6)][PCO] was dissolved in 1,2-dichlorobenzene (1,2-DCB) in an NMR tube, and one equivalent of CS_2 was added with a microsyringe. This solution immediately darkened from yellow to orange, and ^{31}P NMR spectroscopy revealed a singlet resonance at δ = –118.0 ppm, which is consistent with the clean and quantitative formation of [K(18-crown-6)][PCS] (lithium salt at δ = –121.3 ppm).[42] These solutions can be kept at room temperature for several weeks with no apparent decomposition. The same reaction can be carried out in 1,2-difluorobenzene (1,2-DFB); however, the solution gradually darkens over several hours after addition of CS_2, although product formation is still clean by ^{31}P NMR spectroscopy. We believe that these solvents are particularly effective because 1,2-DCB and 1,2-DFB are both highly polar but also relatively non-coordinating. By comparison, if the reaction is carried out in THF under the same conditions, a copious amount of dark precipitate is rapidly produced and only a very weak signal corresponding to PCS^- is observable in the ^{31}P NMR spectrum after a couple of hours.

Pale yellow needles suitable for single-crystal X-ray diffraction were obtained, and this analysis revealed PCS^- to have a linear triatomic structure with close electrostatic interactions to two neighbouring $[K(18\text{-crown-6})]^+$ cations through the P1 and the S1 atoms (Figure 6). This leads to one-dimensional chains of alternating anions and cations propagating through the lattice, akin to those of [K(18-crown-6)][PCO].[12] However, the P1 and S1 atoms are rendered indistinguishable in the crystal structure due to an inversion centre on the central C1 atom of the anion. This is a manifestation of the comparable C=P and C=S bond lengths and the fact that sulfur and phosphorus are adjacent in the periodic table and therefore have similar X-ray scattering factors. This disorder prevents a meaningful analysis of the bond metric parameters.

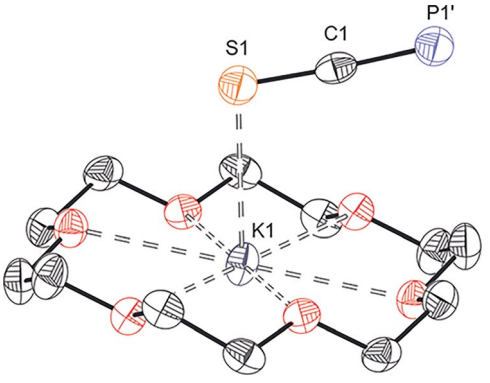

Figure 6. Molecular structure of [K(18-crown-6)][PCS]. Anisotropic displacement ellipsoids are pictured at 50 % probability. All hydrogen atoms are omitted for clarity. Symmetry operation ′: 1 – *x*, 1 – *y*, 1 – *z*.

Analogous reactivity was investigated for the $[Na(1,4\text{-dioxane})_x][PCO]$ salt ($1 < x < 3$). In this case, the starting material is completely insoluble in 1,2-DCB, presumably because of the stable three-dimensional network of octahedrally coordinated Na^+ cations bridged by 1,4-dioxane units.[13] Unsurprisingly, this meant that no reactivity was initially observed upon addition of the CS_2. However, addition of one equivalent of 18-crown-6 to this sample led to the immediate darkening of the reaction mixture and the formation of [Na(18-crown-6)][PCS], as indicated by a singlet resonance at δ = –119.4 ppm in the ^{31}P NMR spectrum. The 18-crown-6 solubilises the starting material by sequestering the Na^+ cations and breaking apart the extended network, leading to reactivity that mirrors the K^+ salt, as expected. For the purposes of consistency, only the reactivity of the $[K(18\text{-crown-6})]^+$ salt of PCS^- will be discussed henceforth {the structure of the $[Na(18\text{-crown-6})]^+$ salt is provided in the Supporting Information}.

Reaction of $W(CO)_5(MeCN)$ with a 1,2-DCB solution of PCS^- led to a darkening of the solution. ^{31}P NMR spectroscopy revealed the slow emergence of two resonances of almost equal intensity either side of the free PCS^- anion after several days (Figure 7). These two resonances occur at –192.6 and –92.9 ppm

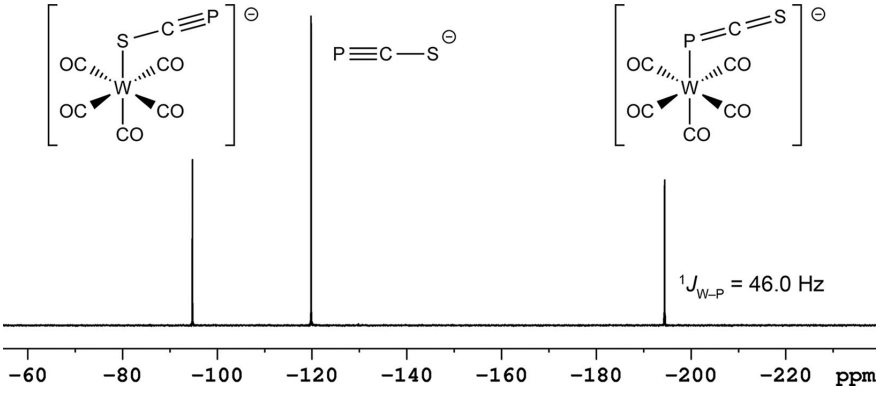

Figure 7. ^{31}P NMR spectrum showing the formation of $[W(CO)_5(PCS)]^-$ (**4a**) and $[W(CO)_5(SCP)]^-$ (**4b**).

and have been attributed to the phosphorus-bound and sulfur-bound species **4a** and **4b**, respectively, due to the ambidentate nature of the PCS^- ligand (vide infra). These were distinguishable by the presence of the ^{183}W satellites on the phosphorus-bound resonance only. The change in chemical shifts relative to free PCS^- is also consistent with this assignment. For **4a**, there is an upfield shift, similar to that observed for [K(18-crown-6)][**1**], while for **4b** a downfield shift is observed, akin to those for the oxygen-bound An–OCP species (An = Th, U) discussed previously. The $^1J_{W\text{-}P}$ coupling constant is only 46.0 Hz, which is a spectroscopic indication that the PCS^- is bound in a side-on manner mainly through a p orbital, as in [K(18-crown-6)][**1**].

Crystals suitable for single-crystal X-ray diffraction were grown by slow diffusion of hexane into a 1,2-DFB solution of the product (Figure 8). Unfortunately, extensive crystallographic disorder makes the unambiguous assignment of the product difficult. The structure certainly contains a PCS^- ligand coordinated to a tungsten–pentacarbonyl centre, but whether it is phosphorus-bound, sulfur-bound, or indeed a combination of the two, is non-trivial, as the residual electron densities change very little between the various refinements. The final solution has been modelled as sulfur-bound, as this gave a slightly lower *R*1(all data) value of 2.29 %.

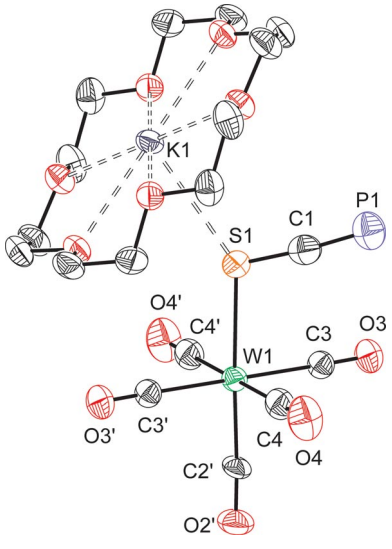

Figure 8. Molecular structure of [K(18-crown-6)][**4b**]. Anisotropic displacement ellipsoids are pictured at 50 % probability, and all hydrogen atoms are omitted for clarity.

The sulfur- and phosphorus-bound products are unstable in 1,2-DCB at room temperature over the course of approximately four days, as monitored by ^{31}P NMR spectroscopy. This, coupled with the fact that PCS^- was very slow at displacing the acetonitrile ligand, meant that this reaction was unsuitable for obtaining a compositionally pure sample of either product. Extensive attempts were made to vary the reaction conditions. Carrying out the reactions at lower temperatures was not a viable option, as this further retarded the already slow rate of coordination. A range of other tungsten–pentacarbonyl precursors were used, including photolysis in the presence of tungsten–hexacarbonyl, but all to no avail. We were further limited by having to carry out the reactions in non-coordinating solvents, which ruled out common derivatives like $W(CO)_5(THF)$. This unfortunately meant that we were not able to explore any further ligand properties of PCS^- experimentally.

Computational Studies

All the ECX^- ligands were studied computationally by DFT with the B3LYP hybrid functional, and the results are in good agreement with experimental observations. Full details of the computational methods employed are provided in the Experimental Section.

The ability of the ECX^- ligands to undergo linkage isomerism, that is, bind through either the E or the X atom, within the $[W(CO)_5(ECX)]^-$ complex was probed. This was done by calculating the difference in energy between the X-bound and E-bound structures: $\Delta E_{link} = E_{X\text{-bound}} - E_{E\text{-bound}}$ (Table 3). In all cases the value is positive, which indicates that all the ECX^- ligands preferably coordinate to the $W(CO)_5$ fragment through the E atom. However, in the case of PCS^- the value is +3.5 kJ mol^{-1}, which is small and within the expected error of the calculations. This supports the earlier spectroscopic observations that the phosphorus- and sulfur-bound species **4a** and **4b** are formed in comparable ratios in the reaction of PCS^- with $W(CO)_5(MeCN)$.

Table 3. The difference in energy between the X-bound and E-bound ECX^- ligands in the $[W(CO)_5(ECX)]^-$ complexes: $\Delta E_{link} = E_{X\text{-bound}} - E_{E\text{-bound}}$.

	ECX^- ligand	ΔE_{link} (kJ mol^{-1})
$1_{calcd.}$	PCO^-	+47.5
$2_{calcd.}$	NCO^-	+54.2
$3_{calcd.}$	NCS^-	+31.4
$4_{calcd.}$	PCS^-	+3.5

Selected computed bond metrics of the five experimentally relevant complexes are presented in Table 4, along with the data for the free ECX^- ligands for comparison. For both PCX^- ligands, phosphorus coordination leads to a lengthening of the P–C bond and a shortening of the C–X bond relative to the free anion. This is consistent with the proposed $[M–P=C=X]^-$ metallaphosphaketene structure and the crystallographic data discussed previously (**A** in Figure 9). Nitrogen coordination for the NCX^- ligands leads to a slight shortening of the N–C and a larger contraction of the C–X bonds. We believe this is more consistent with the formulation $[M–N=C=X]^-$ (**B1**), although

Table 4. Selected computed bond lengths (Å) and angles (°) for free and coordinated ECX^- ligands. The bond angle W–X–C refers to the sulfur-bound **4b** only.

		E–C	C–X	W–E/X–C
PCO^-	free	1.62	1.20	
PCO^-	$1_{calcd.}$	1.64	1.18	99.4
NCO^-	free	1.19	1.22	
NCO^-	$2_{calcd.}$	1.18	1.21	179.2
NCS^-	free	1.18	1.66	
NCS^-	$3_{calcd.}$	1.17	1.64	179.7
PCS^-	free	1.59	1.63	
PCS^-	$4a_{calcd.}$	1.62	1.60	104.0
SCP^-	$4b_{calcd.}$	1.58	1.65	110.0

there will be some contribution from the zwitterionic resonance form $[M–N^{+}\equiv C–X^{-}]^{-}$ (**B2**). If the latter were the major form, a longer C–X bond would be expected in each case. These computational data differ slightly from the crystallographic data for the coordinated NCX^{-} structures [K(2,2,2-crypt)][**2**] and [K(18-crown-6)][**3**]. The crystallographic N–C bonds are shorter than their computational analogues in each case, and the C–X bonds are longer. This suggests that the structures derived crystallographically have a slightly greater contribution from resonance **B2**. This is presumably because the formal negative charge on the X atom in **B2** can be stabilised by the localised K^{+} cation, whereas these interactions are not present in the computational structures. When the PCS^{-} ligand binds through the sulfur atom, the P–C bond shortens and the C–S bond lengthens relative to the free anion. This is consistent with resonance structure **C** containing a formal P≡C–S fragment (Figure 9).

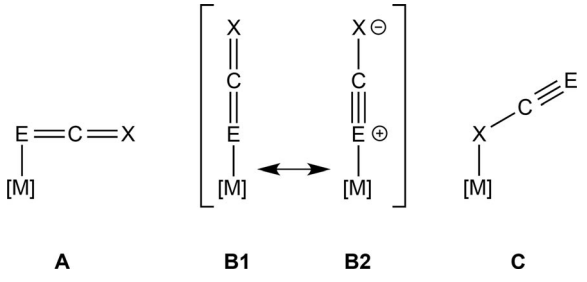

Figure 9. Resonance structures for ECX^{-} fragments bound to a metal centre.

The optimised structures for $\mathbf{1}_{calcd.}$ and $\mathbf{4a}_{calcd.}$ show that both PCX^{-} species are bound side-on, with W–E–C bond angles of 99.4° and 104.0°, respectively. When the PCX^{-} anions were repositioned to an end-on geometry, and the optimisation was constrained to C_{4v} symmetry, the optimised geometries each gave two imaginary frequencies (a second order saddle point), which correspond to two symmetric relaxations to the side-on geometry. This is consistent with the rehybridisation of the phosphorus atom to a lone pair of electrons and the concomitant loss of some of the multiple bond character of the P–C bond. The difference in energy between the two conformational isomers was calculated as $\Delta E_{con} = E_{end\text{-}on} - E_{side\text{-}on}$ and gave values of +65.9 and +38.5 kJ mol^{-1} for PCO^{-} and PCS^{-}, respectively. This shows that the side-on bonding mode is thermodynamically favoured for the PCX^{-} ligands and not simply a result of crystal packing. The smaller ΔE_{con} for PCS^{-} relative to PCO^{-} can be rationalised by considering the allene-like structure **A** of the side-on ligand. In both cases, there is a decrease in the P–C multiple bond character from the linear structure **B**, but there is also an increase in the C–X multiple bond character. It is simply less favourable to form multiple C=S bonds than C=O bonds as a result of the poorer overlap and energy match of the orbitals involved.

The pentacarbonyltungsten fragment is also an ideal fragment for the assessment of ligand properties by using IR spectroscopy. $W(CO)_5(PR_3)$ systems have been used extensively to study the bonding nature of phosphines as a safer alternative to those derived from the toxic $Ni(CO)_4$ used by Tolman in his seminal studies.[39,44] The tungsten–carbonyl stretching frequencies for $[W(CO)_5(ECX)]^{-}$ have been calculated and compared to experimental solid-state data for the $[K(18\text{-crown-}6)]^{+}$ salts where possible (Table 5). Note that no correction factors have been applied to the computational values, but qualitative discussions of trends are still poignant. The force constants for the *cis* and *trans* carbonyl groups have also been calculated for both computational and experimental cases by using the method published by Cotton and Kraihanzel.[43]

Table 5. Computed and experimental tungsten-bound CO stretching frequencies for $[W(CO)_5(ECX)]^{-}$ (cm^{-1}) and Cotton–Kraihanzel force constants (mdyne Å^{-1}).[43]

	PCO^{-}	NCO^{-}	NCS^{-}	PCS^{-}
$A_1^{(1)}$	2107	2115	2119	2108
$A_1^{(1)}$ (exptl.)	2047	2064	2065	
B_1	2000	2003	2010	2006
B_1 (exptl.)	1970	1966	1980	
E	1948	1946	1954	1954
E (exptl.)	1917	1902	1906	
$A_1^{(2)}$	1895	1883	1900	1901
$A_1^{(2)}$ (exptl.)	1858	1823	1851	
k_1 (*trans*)	14.70	14.52	14.79	14.79
k_1 (*trans*) (exptl.)	14.09	13.60	14.03	
k_2 (*cis*)	16.13	16.15	16.25	16.20
k_2 (*cis*) (exptl.)	15.48	15.41	15.46	

The symmetry labels in Table 5 for the stretching frequencies are strictly for $W(CO)_5(L)$ structures with C_{4v} symmetry, in which case the B_1 frequency would not be visible in the IR spectrum. In all cases this is slightly relaxed, though the structures for $\mathbf{2}_{calcd.}$ and $\mathbf{3}_{calcd.}$ are very close, and the B_1 band is extremely weak. Structures $\mathbf{1}_{calcd.}$ and $\mathbf{4a}_{calcd.}$ both have C_s symmetry, which also lifts the degeneracy of the E band (separation less than 2 cm^{-1}), so an average value is given. In all the experimental structures the symmetry is lowered by the interaction of the anion with the $[K(18\text{-crown-}6)]^{+}$ cation, so the anion can never truly be considered separately. However, all the anions are pseudo-C_{4v} and are treated as such for this discussion.

As can be seen in Table 5, all of the ECX^{-} ligands exert comparable effects on the IR spectra of complexes **1**–**4**, despite significant variations in the coordination modes of the phosphorus- and nitrogen-containing species. The recorded CO stretching frequencies differ by no more than 12 cm^{-1}, which indicates that the net *trans* influence of the ligands is largely the same. These data and the $^{1}J_{W\text{-}C(trans)}$ coupling constant values discussed earlier strongly suggest that the nitrogen-containing ligands, NCO^{-} and NCS^{-}, possess increased π-acceptor properties compared to those of their heavier phosphorus-containing analogues. This offsets their greater σ-donor ability, making the overall effect on the electron density of the metal centre comparable for all of the ligands studied.

Conclusions

We have extensively explored the ligand properties of PCO^{-} compared to those of NCO^{-}, both experimentally and computationally. We report the first synthesis of PCS^{-} under ambient conditions, and the ligand study was extended to include ECS^{-} (E = N, P).

We can confirm that PCX^{-} species preferentially bind in a side-on manner, in contrast to their NCX^{-} analogues. Further-

more, the observation of weak $^1J_{W\text{-}P}$ coupling constant values show that these bent conformations are maintained in solution and that terminal (linear) PCX^- structures are largely unfavourable. This was further confirmed by DFT calculations.

Interestingly, a comparison of PCO^- and NCO^- ligands has shown that, while the two ligands exert a comparable *trans* influence on the carbonyl substituent (as evidenced by structural and IR spectroscopic data), this effect arises from the fundamentally different electronic properties of the ligands and their respective bonding modes. Thus, we conclude that PCO^- is a significantly weaker σ-donor ligand than NCO^-; however, as a result of both the coordination geometry of NCO^- and its electronic structure, the increased π-acceptor properties give the two ligands the same net properties. Further studies on the coordination chemistry and reactivity of the coordinated PCX^- anions are currently on-going and bode well for the generation of novel phosphorus-containing small molecules.

Experimental Section

General Synthetic Methods and Reagents

All reactions and product manipulations were carried out under an inert atmosphere of argon or dinitrogen by using standard Schlenk or glovebox techniques (MBraun UNILab glovebox maintained at less than 0.1 ppm O_2 and less than 0.1 ppm H_2O) unless otherwise specified.

Potassium cyanate (KOCN; Sigma Aldrich, 96 %), potassium thiocyanate (KSCN; Sigma Aldrich, ≥ 99 %), tungsten–hexacarbonyl [$W(CO)_6$; Acros Organics, 99 %], carbon disulfide (CS_2; Sigma Aldrich, anhydrous ≥ 99 %) and $Me_3NO{\cdot}2H_2O$ (Alfa Aesar, 98+%) were all used as received. 18-Crown-6 (1,4,7,10,13,16-hexaoxacyclooctadecane; Alfa Aesar, 99 %) and 2,2,2-crypt (4,7,13,16,21,24-hexaoxa-1,10-diazabicyclo[8,8,8]-hexacosane; VWR, 99 %) were used as received after careful drying under vacuum.

Tetrahydrofuran (THF; Fisher, HPLC grade) was distilled from a sodium/benzophenone mixture. Acetonitrile (Sigma Aldrich, CHROMASOLV® gradient grade for HPLC, ≥ 99.9 %), hexane (Sigma Aldrich, HPLC grade) and toluene (Sigma Aldrich, HPLC grade) were purified by using an MBraun SPS-800 solvent system. [D_8]THF (Eurisotop >99.5 %) was dried with CaH_2, vacuum distilled and degassed before use. All dry solvents were stored under argon in gas-tight ampoules. Additionally, hexane, THF, [D_8]THF and toluene were stored over activated 3 Å molecular sieves. 1,2-Dichlorobenzene (1,2-DCB; Sigma Aldrich, anhydrous 99 %), 1,2-difluorobenzene (1,2-DFB; Fluorochem, 98 %) and [D_4]1,2-dichlorobenzene {[D_4]1,2-DCB; Alfa Aesar, 99 % (isotopic)} were dried and stored over activated 3 Å sieves and degassed before use. [Na(dioxane)$_{2.69}$][PCO],[21] [K(18-crown-6)][PCO][12] and $W(CO)_5$(MeCN)[45] were prepared according to literature methods.

[K(18-crown-6)][$W(CO)_5$(PCO)] ([K(18-crown-6)][1]): Solid [K(18-crown-6)][PCO] (170 mg, 0.47 mmol) was added to a stirring yellow THF solution (30 mL) of $W(CO)_5$(MeCN) (259 mg, 0.71 mmol). The solution darkened to an orange colour over the course of 30 minutes, then the volatiles were removed in vacuo to leave an oily yellow/orange solid. This was washed with toluene (3 × 5 mL), then dried in vacuo to afford a yellow/orange solid of compositionally pure [K(18-crown-6)][**1**]. Yield: 161 mg (50 % with respect to P). Orange crystals suitable for single-crystal X-ray diffraction were grown by slow diffusion of hexane into a THF solution of [K(18-crown-6)][**1**] (CCDC-1412564). $C_{18}H_{24}KO_{12}PW$ (686.30): calcd. C 31.50, H 3.53; found C 31.13, H 3.53. ^{1}H NMR (500 MHz, [D_8]-THF, 298 K): δ = 3.63 (s, 18-crown-6) ppm. ^{31}P NMR (202.4 MHz, [D_8]THF, 298 K): δ = –439.3 (s, sat, $^1J_{W\text{-}P}$ = 51.9 Hz) ppm. ^{13}C{^{1}H} NMR (125.8 MHz, [D_8]THF, 298 K): δ = 204.6 (d, $^2J_{C\text{-}P}$ = 9.4, sat, $^1J_{W\text{-}C}$ = 168.6 Hz; *trans*-CO), 202.1 (d, $^2J_{C\text{-}P}$ = –3.7, sat, $^1J_{W\text{-}C}$ = 125.4 Hz; *cis*-CO), 173.0 (d, $^1J_{C\text{-}P}$ = 94.7 Hz; PCO), 71.3 (s; 18-crown-6) ppm. IR (Nujol mull): $\tilde{\nu}$(CO) = 2047 (w, A_1), 1970 (vw, B_1), 1917 (s, E), 1835 (m, A_1) cm^{-1}; $\tilde{\nu}$(PCO) = 1835 (m, asymm.) cm^{-1}.

[K(2,2,2-crypt)][$W(CO)_5$(PCO)] ([K(2,2,2-crypt)][1]): Solid [K(18-crown-6)][PCO] (288 mg, 0.80 mmol) was added to a stirring yellow THF solution (30 mL) of $W(CO)_5$(MeCN) (290 mg, 0.80 mmol). After 20 minutes of stirring, solid 2,2,2-crypt (300 mg, 0.796 mmol) was added. The solution was left to stir for another 30 minutes, after which the volatiles were removed in vacuo to leave an oily orange solid. This was washed with toluene (1 × 10 mL) and pentane (2 × 10 mL), and then dried under a dynamic vacuum to afford an orange solid of [K(2,2,2-crypt)][**1**] (467 mg), but also a small amount of uncoordinated PCO^-, as evidenced by ^{31}P NMR spectroscopy. The solid was redissolved in THF (10 mL), and $W(CO)_5$(MeCN) (25 mg) was added. The mixture was stirred for 30 minutes. An orange solid was obtained as before, this time consisting of compositionally pure [K(2,2,2-crypt)][**1**], but with a reduced yield due to the extensive washing. Yield: 220 mg (28 % with respect to P). Orange crystals suitable for single-crystal X-ray diffraction were grown by slow diffusion of hexane into a THF solution of [K(2,2,2-crypt)][**1**] (CCDC-1412565). $C_{24}H_{36}KN_2O_{12}PW$ (798.48): calcd. C 36.10, H 4.54, N 3.51; found C 36.03, H 4.50, N 3.90. ^{1}H NMR (500 MHz, [D_8]THF, 298 K): δ = 3.62 (s, 2,2,2-crypt), 3.58 (m, 2,2,2-crypt), 2.59 (m, 2,2,2-crypt) ppm. ^{31}P NMR (202.4 MHz, [D_8]THF, 298 K): δ = –441.0 (s, sat, $^1J_{W\text{-}P}$ = 51.8 Hz) ppm. ^{13}C{^{1}H} NMR (125.8 MHz, [D_8]THF, 298 K): δ = 204.6 (d, $^2J_{C\text{-}P}$ = 9.4, sat, $^1J_{W\text{-}C}$ = 167.8 Hz; *trans*-CO), 202.2 (d, $^2J_{C\text{-}P}$ = –3.7, sat, $^1J_{W\text{-}C}$ = 125.5 Hz; *cis*-CO), 173.0 (d, $^1J_{C\text{-}P}$ = 94.9 Hz; PCO), 71.5 (s; 2,2,2-crypt), 68.7 (s; 2,2,2-crypt), 55.1 (s; 2,2,2-crypt) ppm. IR (Nujol mull): $\tilde{\nu}$(CO) = 2052 (w, A_1), 1960 (vw, B_1), 1906 (s, E), 1850 (m, A_1) cm^{-1}; $\tilde{\nu}$(PCO) = 1841 (m, asymm.) cm^{-1}.

[K(18-crown-6)][$W(CO)_5$(NCO)] ([K(18-crown-6)][2]): $W(CO)_6$ (20 mg, 0.06 mmol), KOCN (4.6 mg, 0.06 mmol) and 18-crown-6 (15.0 mg, 0.06 mmol) were weighed into a small gas-tight ampoule and dissolved in THF (5 mL) to give a colourless solution. This was degassed once by means of the freeze-pump-thaw method. The solution was then stirred under irradiation from a mercury lamp (150 W) for 2 h. The bright yellow solution was subsequently transferred to a small Schlenk tube and concentrated in vacuo down to 2 mL. Slow diffusion of hexane into this solution yielded yellow crystals suitable for single-crystal X-ray diffraction, which were solved as [K(18-crown-6)][**2**] (CCDC-1412566). The crystals were subsequently isolated and dried in vacuo. Yield: 28.2 mg (74 % crystalline yield). $C_{18}H_{24}KNO_{12}W$ (669.34): calcd. C 32.30, H 3.61, N 2.09; found C 32.13, H 3.58, N 2.32. ^{1}H NMR (500 MHz, [D_8]-THF, 298 K): δ = 3.63 (s, 18-crown-6) ppm. ^{13}C{^{1}H} NMR (125.8 MHz, [D_8]THF, 298 K): δ = 201.7 (s, sat, $^1J_{W\text{-}C}$ = 146.5 Hz; *trans*-CO), 199.6 (s, sat, $^1J_{W\text{-}C}$ = 127.8 Hz; *cis*-CO), 129.9 (br; NCO), 71.3 (s; 18-crown-6) ppm. IR (Nujol mull): $\tilde{\nu}$(CO) = 2064 (w, A_1), 1966 (vw, B_1), 1902 (s, E), 1823 (m, A_1) cm^{-1}; $\tilde{\nu}$(NCO) = 2241 (m, asymm.) cm^{-1}.

[K(2,2,2-crypt)][$W(CO)_5$(NCO)] ([K(2,2,2-crypt)][2]): $W(CO)_5$(MeCN) (300 mg, 0.82 mmol), KOCN (44.5 mg, 0.548 mmol) and 2,2,2-crypt (206.4 mg, 0.55 mmol) were dissolved in THF (30 mL) and stirred for one hour to give a yellow/brown solution. Volatiles were removed in vacuo to give a yellow/brown solid. This was washed with toluene (3 × 10 mL) to afford a yellow solid. Yield: 320 mg (75 %). Yellow crystals suitable for single-crystal X-ray dif-

fraction were grown by slow diffusion of hexane into a THF solution of [K(2,2,2-crypt)][**2**] (CCDC-1412567). $C_{24}H_{36}KN_3O_{12}W$ (781.51): calcd. C 36.89, H 4.64, N 5.38; found C 36.93, H 4.53, N 5.38. ^{1}H NMR (500 MHz, [D$_8$]THF, 298 K): δ = 3.61 (s, 2,2,2-crypt), 3.56 (m, 2,2,2-crypt), 2.58 (m, 2,2,2-crypt) ppm. ^{13}C{^{1}H} NMR (125.8 MHz, [D$_8$]THF, 298 K): δ = 201.7 (s, sat, $^1J_{W\text{-}C}$ = 146.6 Hz; *trans*-CO), 199.6 (s, sat, $^1J_{W\text{-}C}$ = 127.7 Hz; *cis*-CO), 130.2 (br; NCO), 71.5 (s; 2,2,2-crypt), 68.7 (s; 2,2,2-crypt), 55.1 (s; 2,2,2-crypt) ppm. IR (Nujol mull): $\tilde{\nu}$(CO) = 2062 (w, A$_1$), 1965 (vw, B$_1$), 1912 (s, E), 1831 (m, A$_1$) cm^{-1}; $\tilde{\nu}$(NCO) = 2240 (m, asymm.) cm^{-1}.

[K(18-crown-6)][W(CO)$_5$(NCS)] ([K(18-crown-6)][3]): W(CO)$_5$(MeCN) (308 mg, 0.84 mmol), KSCN (86 mg, 0.84 mmol) and 18-crown-6 (234 mg, 0.84 mmol) were stirred in THF (30 mL) for one hour to give a yellow solution with undissolved white solid. EtOH (30 mL) was added, and this gave the desired yellow solution with no precipitate. This was left to stir for a further hour. Volatiles were removed under a dynamic vacuum to give a yellow solid. This was washed with toluene (1 × 20 mL) to afford a yellow solid. Yield: 396 mg (65 %). Yellow crystals suitable for single-crystal X-ray diffraction were grown by slow diffusion of hexane into a THF solution of [K(18-crown-6)][**3**] (CCDC-1412568). $C_{18}H_{24}KNO_{11}SW$ (685.40): calcd. C 31.54, H 3.53, N 2.04; found C 31.50, H 3.54, N 2.02. ^{1}H NMR (500 MHz, [D$_8$]THF, 298 K): δ = 3.65 (s, 18-crown-6) ppm. ^{13}C{^{1}H} NMR (125.8 MHz, [D$_8$]THF, 298 K): δ = 201.3 (s, sat, $^1J_{W\text{-}C}$ = 147.7 Hz; *trans*-CO), 198.8 (s, sat, $^1J_{W\text{-}C}$ = 128.3 Hz; *cis*-CO), 139.6 (br; NCS), 71.4 (s; 18-crown-6) ppm. IR (Nujol mull): $\tilde{\nu}$(CO) = 2065 (w, A$_1$), 1980 (vw, B$_1$), 1906 (s, E), 1851 (m, A$_1$) cm^{-1}; $\tilde{\nu}$(NCS) = 2106 (m, asymm.) cm^{-1}.

[K(18-crown-6)][PCS]: [K(18-crown-6)][PCO] (30 mg, 0.08 mmol) was dissolved in 1,2-DCB (5 mL) to give a yellow solution. CS_2 (5 µL, 0.08 mmol) was added with a microsyringe, and the mixture was stirred for 30 minutes to give an orange solution. The volatiles were removed in vacuo to yield an orange solid. This was redissolved in 1,2-DCB (2 mL), and the volatiles were subsequently removed in vacuo again to yield a free-flowing orange solid. Yield: 31.2 mg (99 %). Crystals suitable for single-crystal X-ray diffraction were grown by slow diffusion of hexane into a 1,2-DFB solution of [K(18-crown-6)][PCS] (CCDC-1412569). $C_{13}H_{24}KO_6PS$ (378.46): calcd. C 41.26, H 6.39; found C 40.67, H 6.18. ^{1}H NMR (499.9 MHz, [D$_4$]1,2-DCB, 298 K): δ = 3.40 (s; 18-crown-6) ppm. ^{31}P NMR (202.4 MHz, 1,2-[D$_4$]DCB, 298 K): δ = –118.0 (s) ppm. ^{13}C{^{1}H} NMR (125.8 MHz, [D$_4$]1,2-DCB, 298 K): δ = 191.3 (d, $^1J_{C\text{-}P}$ = 20.7 Hz; PCS), 70.2 (s; 18-crown-6) ppm.

[Na(18-crown-6)][PCS]: [Na(dioxane)$_{2.69}$][PCO] (100 mg, 0.313 mmol) and 18-crown-6 (82.9 mg, 0.313 mmol) were dissolved in 1,2-DCB (5 mL) to give a yellow solution. CS_2 (18.9 µL, 0.313 mmol) was added with a microsyringe, and the mixture was stirred overnight to give an orange solution. ^{31}P NMR spectroscopy of a 0.5 mL aliquot showed quantitative conversion to [Na(18-crown-6)][PCS]. The volatiles were removed in vacuo to yield an orange solid. The solid was redissolved in 1,2-DCB (5 mL) and used to obtain crystals suitable for single-crystal X-ray diffraction, which were grown by slow diffusion of hexane into the 1,2-DCB solution of [Na(18-crown-6)][PCS] in a fridge at 4 °C (CCDC-1412570). ^{31}P NMR (202.4 MHz, 1,2-DCB, 298 K): δ = –119.4 (s) ppm.

Reaction of [K(18-crown-6)][PCS] and W(CO)$_5$(MeCN) (Synthesis of 4a and 4b): A 1,2-DFB solution (30 mL) of [K(18-crown-6)][PCS] (209 mg, 0.552 mol) was added to a stirring yellow 1,2-DFB solution (20 mL) of W(CO)$_5$(MeCN) (201 mg, 0.552 mmol) at 0 °C and slowly warmed up to room temperature. The solution went dark over the course of an hour. The reaction was monitored by ^{31}P NMR spectroscopy, which showed the growth of two new resonances in addition to that of free PCS$^-$, which have been attributed to products **4a** (P-bound) and **4b** (S-bound). After four days at room temperature, there were no signals in the ^{31}P NMR spectrum. Single crystals were grown by slow diffusion of hexane into a 1,2-DFB solution of a mixture of **4a** and **4b**, but the crystals exhibited extensive crystallographic disorder, which precluded any detailed analysis (CCDC-1412571). ^{31}P NMR (202.4 MHz, 1,2-DFB, 298 K): δ = –92.9 (s; [W(CO)$_5$(SCP)]$^-$), –192.6 (s, sat, $^1J_{W\text{-}P}$ = 46.0 Hz; [W(CO)$_5$(PCS)]$^-$) ppm.

Analytical Methods

^{1}H, ^{13}C and ^{31}P NMR spectra were acquired at 500.0, 125.8 and 202.4 MHz, respectively, with a Bruker AVIII 500 MHz NMR spectrometer. ^{1}H and ^{13}C NMR spectra are reported relative to Si(CH$_3$)$_4$ (δ_H = 0 ppm, δ_C = 0 ppm) and were referenced to residual solvent resonances ([D$_8$]THF: δ_H = 3.58 ppm, δ_C = 67.57 ppm; [D$_4$]1,2-DCB: δ_H = 6.93 ppm, δ_C = 132.4 ppm). ^{31}P NMR spectra were externally referenced to 85 % H_3PO_4 (δ_P = 0 ppm). All spectra were obtained at 25 °C. Data were processed by using the Bruker TopSpin 3.1 program.

IR spectroscopic data were recorded by using solid samples in a Nujol mull. Samples were prepared inside an inert-atmosphere glovebox, and the KBr plates were placed in an airtight sample holder prior to data collection. Spectra were recorded with a Thermo Scientific iS5 FTIR spectrometer in absorbance mode.

Single-crystal X-ray diffraction data were collected by using either an Oxford Diffraction Supernova dual-source diffractometer equipped with a 135 mm Atlas CCD area detector or an Enraf–Nonius kappa-CCD diffractometer equipped with a 95 mm CCD area detector. Crystals were selected under Paratone-N oil, mounted on micromount loops and quench-cooled with an Oxford Cryosystems open-flow N_2 cooling device.[46] Data were collected at 150 K by using mirror monochromated Cu-K_α radiation (λ = 1.5418 Å; Oxford Diffraction Supernova) or graphite-monochromated Mo-K_α radiation (λ = 0.71073 Å; Enraf–Nonius kappa-CCD). Data collected with the Oxford Diffraction Supernova diffractometer were processed by using the CrysAlisPro package, including unit cell parameter refinement and interframe scaling (which was carried out by using SCALE3 ABSPACK within CrysAlisPro).[47] Equivalent reflections were merged, and diffraction patterns were processed with the CrysAlisPro suite. For data collected on the Enraf–Nonius kappa-CCD diffractometer, equivalent reflections were merged and the diffraction patterns were processed with the DENZO and SCALEPACK programs.[48] Structures were subsequently solved by direct methods or by using the charge flipping algorithm, as implemented in the program SUPERFLIP,[49] and refined on F^2 with the SHELXL 97–2 package.[50]

CCDC-1412564 (for [K(18-crown-6)][**1**]), -1412565 (for [K(2,2,2-crypt)][**1**]), -1412566 (for [K(18-crown-6)][**2**]), -1412567 (for [K(2,2,2-crypt)][**2**]), -1412568 (for [K(18-crown-6)][**3**]), -1412569 (for [K(18-crown-6)][PCS]), -1412570 (for [Na(18-crown-6)][PCS]) and -1412571 (for [K(18-crown-6)][**4**]) contain the supplementary crystallographic data for this paper. These data can be obtained free of charge from The Cambridge Crystallographic Data Centre via www.ccdc.cam.ac.uk/data_request/cif.

Computational Details: All DFT calculations were performed by using the Gaussian09 software package.[51] The B3LYP functional was used throughout,[52] with the 6-311+G(2df,p) basis set on all atoms except for tungsten,[53] which was treated with a Stuttgart/Dresden Effective Core Potential (ECP).[54] Solvent interactions (tetrahydrofuran) were treated implicitly with a polarisable continuum model.[55] The nature of stationary points was confirmed by frequency analysis: in all cases all frequencies were real except for

the geometries constrained to C_{4v} symmetry, each one of which displayed two imaginary frequencies. All quantum chemical results were visualised by using the Chemcraft 1.7 software.[56]

Acknowledgments

We thank the Engineering and Physical Sciences Research Council (EPSRC) and the University of Oxford for financial support of this research (DTA studentship to A. R. J.) and the University of Oxford for access to Chemical Crystallography and Advanced Research Computing (ARC) facilities. We also thank Elemental Microanalysis Ltd (Devon) for performing the elemental analyses.

Keywords: Coordination modes · Ligand effects · P ligands · Cyanates · Thiocyanates

[1] K. S. Pitzer, *J. Am. Chem. Soc.* **1948**, *70*, 2140–2145.
[2] P. Jutzi, *Angew. Chem. Int. Ed. Engl.* **1975**, *14*, 232–245; *Angew. Chem.* **1975**, *87*, 269.
[3] a) K. B. Dillon, F. Mathey, J. F. Nixon, *Phosphorus: The Carbon Copy*, John Wiley and Sons, New York, **1998**; b) F. G. A. Stone, R. West (Eds.), *Multiply Bonded Main Group Metals and Metalloids (Advances in Organometallic Chemistry, Volume 39)*, Academic Press, San Diego, **1996**; c) P. P. Power, *J. Chem. Soc., Dalton Trans.* **1998**, 2939–2951; d) S. T. Liddle (Ed.), *Molecular Metal–Metal Bonds: Compounds, Synthesis Properties*, Wiley-VCH, Weinheim, **2015**.
[4] M. Yoshifuji, I. Shima, N. Inamoto, K. Hirotsu, T. Higuchi, *J. Am. Chem. Soc.* **1981**, *103*, 4587–4589.
[5] T. C. Klebach, R. Lourens, F. Bickelhaupt, *J. Am. Chem. Soc.* **1978**, *100*, 4886–4888.
[6] T. A. Van Der Knaap, T. C. Klebach, F. Visser, F. Bickelhaupt, P. Ros, E. J. Baerends, C. H. Stam, M. Konijn, *Tetrahedron* **1984**, *40*, 765–776.
[7] O. Mundt, G. Becker, W. Uhl, W. Massa, M. Birkhahn, *Z. Anorg. Allg. Chem.* **1986**, *540*, 319–335.
[8] G. Becker, G. Gresser, W. Uhl, *Z. Naturforsch. B* **1981**, *36*, 16–19.
[9] G. Becker, W. Schwarz, N. Seidler, M. Westerhausen, *Z. Anorg. Allg. Chem.* **1992**, *612*, 72–82.
[10] L. Weber, B. Torwiehe, G. Bassmann, H.-G. Stammler, B. Neumann, *Organometallics* **1996**, *15*, 128–132.
[11] G. Becker, G. Heckmann, K. Hübler, W. Schwarz, *Z. Anorg. Allg. Chem.* **1995**, *621*, 34–46.
[12] A. R. Jupp, J. M. Goicoechea, *Angew. Chem. Int. Ed.* **2013**, *52*, 10064–10067; *Angew. Chem.* **2013**, *125*, 10248–10251.
[13] F. F. Puschmann, D. Stein, D. Heift, C. Hendriksen, Z. A. Gal, H.-F. Grützmacher, H. Grützmacher, *Angew. Chem. Int. Ed.* **2011**, *50*, 8420–8423; *Angew. Chem.* **2011**, *123*, 8570–8574.
[14] A. R. Jupp, J. M. Goicoechea, *J. Am. Chem. Soc.* **2013**, *135*, 19131–19134.
[15] M. B. Geeson, A. R. Jupp, J. E. McGrady, J. M. Goicoechea, *Chem. Commun.* **2014**, *50*, 12281–12284.
[16] A. R. Jupp, G. Trott, É. Payen de la Garanderie, J. D. G. Holl, D. Carmichael, J. M. Goicoechea, *Chem. Eur. J.* **2015**, *21*, 8015–8018.
[17] T. P. Robinson, J. M. Goicoechea, *Chem. Eur. J.* **2015**, *21*, 5727–5731.
[18] X. Chen, S. Alidori, F. F. Puschmann, G. Santiso-Quinones, Z. Benkő, Z. Li, G. Becker, H.-F. Grützmacher, H. Grützmacher, *Angew. Chem. Int. Ed.* **2014**, *53*, 1641–1645; *Angew. Chem.* **2014**, *126*, 1667–1671.
[19] D. Heift, Z. Benkő, H. Grützmacher, *Angew. Chem. Int. Ed.* **2014**, *53*, 6757–6761; *Angew. Chem.* **2014**, *126*, 6875–6879.
[20] D. Heift, Z. Benkő, H. Grützmacher, *Chem. Eur. J.* **2014**, *20*, 11326–11330.
[21] D. Heift, Z. Benkő, H. Grützmacher, *Dalton Trans.* **2014**, *43*, 831–840.
[22] D. Heift, Z. Benkő, H. Grützmacher, A. R. Jupp, J. M. Goicoechea, *Chem. Sci.* **2015**, *6*, 4017–4024.
[23] T. P. Robinson, M. J. Cowley, D. Scheschkewitz, J. M. Goicoechea, *Angew. Chem. Int. Ed.* **2015**, *54*, 683–686; *Angew. Chem.* **2015**, *127*, 693–696.
[24] A. M. Tondreau, Z. Benkő, J. R. Harmer, H. Grützmacher, *Chem. Sci.* **2014**, *5*, 1545–1554.
[25] C. Camp, N. Settineri, J. Lefèvre, A. R. Jupp, J. M. Goicoechea, L. Maron, J. Arnold, *Chem. Sci.* **2015**, *6*, 6379–6384.
[26] D. Heift, Z. Benkő, H. Grützmacher, *Dalton Trans.* **2014**, *43*, 5920–5928.
[27] S. Alidori, D. Heift, G. Santiso-Quinones, Z. Benkő, H. Grützmacher, M. Caporali, L. Gonsalvi, A. Rossin, M. Peruzzini, *Chem. Eur. J.* **2012**, *18*, 14805–14811.
[28] W. Beck, H. S. Smedal, *Angew. Chem. Int. Ed. Engl.* **1966**, *5*, 253–253; *Angew. Chem.* **1966**, *78*, 267.
[29] R. M. Dahlgren, J. I. Zink, *J. Am. Chem. Soc.* **1979**, *101*, 1448–1454.
[30] K. J. Asali, G. R. Dobson, *J. Organomet. Chem.* **1979**, *179*, 169–179.
[31] M. Herberhold, W. Ehrenreich, *Angew. Chem. Int. Ed. Engl.* **1982**, *21*, 633–633; *Angew. Chem.* **1982**, *94*, 637.
[32] W. Palitzsch, C. Beyer, U. Böhme, B. Rittmeister, G. Roewer, *Eur. J. Inorg. Chem.* **1999**, 1813–1820.
[33] A. Wojcicki, M. F. Farona, *J. Inorg. Nucl. Chem.* **1964**, *26*, 2289–2290.
[34] W. Buchner, W. A. Schenk, *Inorg. Chem.* **1984**, *23*, 132–137.
[35] A. Wojcicki, M. F. Farona, *Inorg. Chem.* **1964**, *3*, 151–152.
[36] B. Albert, M. Jansen, *Z. Anorg. Allg. Chem.* **1995**, *621*, 464–468.
[37] For 782 crystallographically characterised complexes of tungsten–pentacarbonyl bearing a phosphorus-bound ligand (CSD version 5.36, June 2015): d_{min} = 2.375 Å, d_{max} = 2.686 Å, d_{mean} = 2.513 Å, Var(d) = 0.002, $\sigma(d)$ = 0.047 Å, mean deviation = 0.037 Å.
[38] J. Pickardt, L. Rösch, H. Schumann, *Z. Anorg. Allg. Chem.* **1976**, *426*, 66–76.
[39] C. A. Tolman, *J. Am. Chem. Soc.* **1970**, *92*, 2956–2965.
[40] H. Schumann, H.-J. Kroth, *Z. Naturforsch. B* **1977**, *32b*, 768–770.
[41] J. K. Burdett, T. A. Albright, *Inorg. Chem.* **1979**, *18*, 2112–2120.
[42] G. Becker, K. Hübler, *Z. Anorg. Allg. Chem.* **1994**, *620*, 405–417.
[43] F. A. Cotton, C. S. Kraihanzel, *J. Am. Chem. Soc.* **1962**, *84*, 4432–4438.
[44] C. A. Tolman, *Chem. Rev.* **1977**, *77*, 313–348.
[45] F. Nief, F. Mercier, F. Mathey, *J. Organomet. Chem.* **1987**, *328*, 349–355.
[46] J. Cosier, A. M. Glazer, *J. Appl. Crystallogr.* **1986**, *19*, 105–107.
[47] *CrysAlisPro*, Agilent Technologies, Version 1.171.35.8.
[48] Z. Otwinowski, W. Minor, *Macromol. Crystallogr., Part A* **1997**, *276*, 307–326.
[49] L. Palatinus, G. Chapius, *J. Appl. Crystallogr.* **2007**, *40*, 786–790.
[50] a) G. M. Sheldrick in *SHELXL97, Programs for Crystal Structure Analysis (Release 97–2)*, Institut für Anorganische Chemie der Universität, Tammanstrasse 4, 3400 Göttingen, Germany, **1998**; b) G. M. Sheldrick, *Acta Crystallogr., Sect. A* **1990**, *46*, 467–473; c) G. M. Sheldrick, *Acta Crystallogr., Sect. A* **2008**, *64*, 112–122.
[51] M. J. Frisch, G. W. Trucks, H. B. Schlegel, G. E. Scuseria, M. A. Robb, J. R. Cheeseman, G. Scalmani, V. Barone, B. Mennucci, G. A. Petersson, H. Nakatsuji, M. Caricato, X. Li, H. P. Hratchian, A. F. Izmaylov, J. Bloino, G. Zheng, J. L. Sonnenberg, M. Hada, M. Ehara, K. Toyota, R. Fukuda, J. Hasegawa, M. Ishida, T. Nakajima, Y. Honda, O. Kitao, H. Nakai, T. Vreven, J. A. Montgomery Jr., J. E. Peralta, F. Ogliaro, M. Bearpark, J. J. Heyd, E. Brothers, K. N. Kudin, V. N. Staroverov, R. Kobayashi, J. Normand, K. Raghavachari, A. Rendell, J. C. Burant, S. S. Iyengar, J. Tomasi, M. Cossi, N. Rega, J. M. Millam, M. Klene, J. E. Knox, J. B. Cross, V. Bakken, C. Adamo, J. Jaramillo, R. Gomperts, R. E. Stratmann, O. Yazyev, A. J. Austin, R. Cammi, C. Pomelli, J. W. Ochterski, R. L. Martin, K. Morokuma, V. G. Zakrzewski, G. A. Voth, P. Salvador, J. J. Dannenberg, S. Dapprich, A. D. Daniels, Ö. Farkas, J. B. Foresman, J. V. Ortiz, J. Cioslowski, D. J. Fox, *Gaussian 09, Revision A.02*, Gaussian, Inc., Wallingford CT, **2009**.
[52] A. D. Becke, *J. Chem. Phys.* **1993**, *98*, 5648–5652.
[53] A. D. McLean, G. S. Chandler, *J. Chem. Phys.* **1980**, *72*, 5639–5648.
[54] D. Andrae, U. Häußermann, M. Dolg, H. Stoll, H. Preuß, *Theor. Chim. Acta* **1990**, *77*, 123–141.
[55] A. Klamt, *J. Phys. Chem.* **1995**, *99*, 2224–2235.
[56] G. A. Zhurko, *ChemCraft v1.7 (build 382)*; www.chemcraftprog.com.

Received: September 21, 2015
Published Online: November 4, 2015